Research Square

Preprints are preliminary reports that have not undergone peer review.
They should not be considered conclusive, used to inform clinical practice,
or referenced by the media as validated information.

Subtypes of corneal neuropathy progression in Parkinson's disease and their association with clinical phenotypes

Chenyang Guan
Xuzhou Medical University
Zixuan Wu
Xuzhou Medical University
Liying Yang
Xuzhou Medical University
Xiaojie Qi
Xuzhou Medical University
Zihao Lin
Xuzhou Medical University
Yating Fang
Xuzhou Medical University
Zhuoxuan Yu
Xuzhou Medical University
Yangdanyu Li
Xuzhou Medical University
KUPPAM SAI SAGAR
Xuzhou Medical University
SHAHRUKH KHAN
Xuzhou Medical University
Peixiao Yin
Xuzhou Medical University
Xuebin Niu
Xuzhou Medical University
He Wang
Xuzhou Medical University
Lu Chen
Xuzhou Medical University
Jing Liu
Xuzhou Medical University
Guiyun Cui

Xuzhou Medical University

Lishun Xiao

Xuzhou Medical University

Kun Zan

Xuzhou Medical University

Chuanying Xu

xucy2022@yeah.net

Xuzhou Medical University

Article

Keywords: Parkinson’s disease, Corneal confocal microscopy, Subtype classification, SuStaIn model, Freezing of gait, Biomarker

Posted Date: January 21st, 2026

DOI: https://doi.org/10.21203/rs.3.rs-8587375/v1

License: This work is licensed under a Creative Commons Attribution 4.0 International License.
Read Full License

Additional Declarations: No competing interests reported.

Subtypes of corneal neuropathy progression in Parkinson's disease and their association with clinical phenotypes

Chenyang Guan[ab#], Zixuan Wu[c#], Liying Yang[ab#], Xiaojie Qi[ab], Zihao Lin[ab], Yating Fang[ab], Zhuoxuan Yu[ab], Yangdanyu Li[ab], KUPPAM SAI SAGAR[b], SHAHRUKH KHAN[b], Peixiao Yin[ab], Xuebin Niu[ab], He Wang[e], Lu Chen[e], Jing Liu[d], Guiyun Cui[ab], Lishun Xiao[c*], Kun Zan[ab*], Chuanying Xu[ab*]

[a] Department of Neurology, The Affiliated Hospital of Xuzhou Medical University, Xuzhou, Jiangsu, China

[b] Department of Neurology, The First Clinical College, Xuzhou Medical University, Xuzhou, Jiangsu, China

[c] Department of Biostatistics, School of Public Health, Xuzhou Medical University, Xuzhou, Jiangsu Province, 221004, China

[d] Department of Cell Biology and Neurobiology,Life Sciences College,XuzhouMedical University, Xuzhou, Jiangsu, China

[e] Department of ophthalmology, The Affiliated Hospital of Xuzhou Medical University, Xuzhou, Jiangsu, China

*Corresponding author: Lishun Xiao, Kun Zan and Chuanying Xu

Correspondence: Department of Neurology, The Affiliated Hospital of Xuzhou Medical University, No. 99 Huaihai West Road, Xuzhou, Jiangsu Province, 221000, China

Email: xiaolishun@xzhmu.edu.cn / zankun0608@163.com / xucy2022@yeah.net

Telephone:15862165140

Fax numbers:85601527

# These authors contributed equally to this work and should be considered co-first authors.

Abstract

Parkinson's disease (PD) is characterized by significant clinical heterogeneity, and there is an urgent need for biomarkers that can identify different progression subtypes. This paper utilizes a machine learning technique—Subtype and Stage Inference (SuStaIn)—which can reveal data-driven disease phenotypes with different temporal progression patterns from widely available cross-sectional patient studies. Corneal neuropathy is a promising peripheral biomarker for PD. Based on confocal microscopy of the cornea in PD patients, this study shows that the method can identify subgroups and their unique trajectories of regional neurodegeneration. SuStaIn can identify two subtypes merely through corneal data and uniquely characterize their temporal complexity. Further analysis revealed that these two subtypes correspond to different pathological protein transmission pathways respectively, and showed significant differences on key clinical symptom scales such as UPDRS-II, RBD-HK and FOGQ. The fine-grained patient stratification provided by SuStaIn has significantly enhanced the ability to predict the transformation between diagnostic categories, bringing new hope to the discovery of disease subtypes and precision medicine.

Keywords Parkinson's disease; Corneal confocal microscopy; Subtype classification; SuStaIn model; Freezing of gait; Biomarker

Introduction

Parkinson's disease shows significant heterogeneity in biology. This heterogeneity is mainly manifested in the differences in the distribution and time course of key pathological features such as abnormal aggregation of α -synuclein and degeneration of dopaminergic neurons among individuals, which in turn leads to a high degree of variability in a series of observation indicators ranging from imaging manifestations, humoral biomarkers to clinical behavior assessment. Therefore, in cohort studies, such variability significantly dilutes the statistical effect at the population level and weakens the reliability of a single biomarker as a universal tool for disease diagnosis, staging, or efficacy evaluation[1]. The main causes of this biological heterogeneity can be attributed to two aspects: individuals may follow different pathological origins and transmission paths (i.e., phenotypic heterogeneity), and they are at different time points in the dynamic disease process (i.e., temporal heterogeneity). Previous studies attempting to explain biomarker variations have typically focused only on a single dimension of heterogeneity: either analyzing phenotypic heterogeneity at a rough, often late stage of the disease, or studying temporal heterogeneity in a broad population[2]. However, in Parkinson's disease, due to the difficulty of existing technologies in simultaneously analyzing its complex disease subtype spectrum and the independent evolution trajectories of each subtype over time, the biological insights we have obtained and their application value in patient stratification are both limited. Therefore, constructing a comprehensive Parkinson's disease map that can clearly separate phenotypic heterogeneity from temporal heterogeneity, that is, accurately identifying different disease subtypes and depicting their unique evolutionary paths one by one, has become a core challenge in the current field.

The heterogeneity of PD is clearly reflected in both pathological mechanisms and clinical phenotypes. At the pathological level, α -synuclein aggregates within abnormal neurons may spread between cells in a prion-like manner. Currently, there are mainly two hypothesized

transmission routes, corresponding to different disease subtypes: "body-preferred subtype" and "brain-preferred subtype"[3, 4]. The pathological process of the body's preferred subtype may originate from the peripheral nervous system (such as the intestinal plexus), and then spread to the central nervous system through the sympathetic and vagus nerves. In the early stage, patients mainly present with rapid eye movement sleep behavior disorders, severe autonomic nerve dysfunction (such as constipation), and loss of smell. On the contrary, the pathological process of the brain-preferred subtype may first start in the limbic system or cortex of the brain, or enter and spread through the olfactory bulb. Patients will experience olfactory disorders very early and immediately develop motor symptoms. This difference in pathological origin directly leads to the diversity of clinical manifestations, promoting the research on PD subtypes to evolve from the initial classification based on single motor symptoms to a classification based on multi-domain phenotypes including motor and non-motor symptoms, neuroimaging data, and biochemical markers.

Against this backdrop, it has become crucial to search for in vivo biomarkers that can effectively reflect the pathological processes of the brain and are applicable to fine staging. The cornea, as a special "window" of the central nervous system, provides a new perspective for this. The subepithelial plexus of the cornea is composed of unmyelinated trigeminal nerve sensory fibers, which may have abnormal deposition of α -synuclein, and this is likely to reflect the same pathological process in the brain[5-9]. In addition, its morphological changes (such as reduced nerve fiber density, decreased branches and increased curvature) have been confirmed to be related to the severity and course of PD, providing another dimension of objective quantitative indicators[10, 11]. Therefore, how to integrate these scattered indicators from techniques such as corneal confocal microscopy into a unified staging framework that can simultaneously analyze phenotypic heterogeneity and temporal heterogeneity, and thereby achieve individualized prognosis judgment and precise intervention, has become a key issue that urgently needs to be solved in this field, and is also giving rise to new research paradigms.

This paper introduces Subtype and Stage Inference (SuStaIn), a computational technique that can take into account spatio-temporal heterogeneity to identify population subgroups with common disease progression patterns. This emerging model has been successfully used to

reveal the heterogeneity and temporal complexity of various neurodegenerative diseases, including Alzheimer's disease and frontotemporal dementia. We used a structured corneal confocal microscopy dataset from a PD patient cohort to demonstrate SuStaIn. The results show that SuStaIn can identify subtypes with different degrees of corneal nerve damage from the PD dataset and reconstruct their respective unique future disease time processes. This echoes previous studies in neurodegenerative diseases, demonstrating that individuals exhibit strong consistency with specific SuStaIn subtypes even at very early stages, which contrasts sharply with the "subtype-only models" in the literature that ignore the heterogeneity of disease stages[12].This highlights the potential utility of SuStaIn in the field of precision medicine for PD, especially in achieving early and fine-grained patient stratification(Figure 1).

Method

Clinical and demographic profiles

Among the patients in the Department of Neurology of the Affiliated Hospital of Xuzhou Medical University, Parkinson's disease (PD) was diagnosed according to the clinical diagnostic guidelines formulated by the Society for Movement Disorders (MDS) in 2015[13]. All symptoms were evaluated by the Unified Parkinson's Rating Scale (UPDRS). The healthy control group was composed of volunteers or family members of patients with Parkinson's disease. This study did not include individuals with secondary Parkinson's disease (drug-induced, immune-related, inflammatory, infectious, traumatic or tumor-related) or atypical Parkinson's disease (e.g., progressive supranuclear palsy, corticobasal ganglia regression, multiple system atrophy). Participants under the age of 40 or over 85 were excluded from the study. The exclusion criteria include corneal diseases, thyroid eye diseases, glaucoma, ocular inflammation and previous history of ophthalmic surgery. The clinical data of each participant were thoroughly reviewed by experienced personnel. This study was approved by the Ethics Committee of the Affiliated Hospital of Xuzhou Medical University (XYFY2022-KL 227-01 / XYFY2023-KL 265), and each participant provided informed consent. This study adhered to the principles of clinical research on human subjects as stipulated in the Declaration of Helsinki.

Corneal confocal microscope

Images of the subcorneal plexiform vascular network can be acquired using Heidelberg Retinal Tomography III and Rostock Corneal Plaque (HRT III RCM; Heidelberg Engineering Co., Ltd., Heidelberg, Germany). The current software version is specifically designed to process confocal coaxial microscopy (CCM) images obtained from Heidelberg HRT-III microscopes, featuring a resolution of 384 x 384 pixels and a field of view of 400 x 400 μm² (with resolution calculated as 400/384 = 1.0417 μm). Heidelberg microscopes include an automatic cleaning function for CCM images, which removes the information bar at the bottom of the image, thereby enhancing image clarity. Each eye was anesthetized with lidocaine, and the patient was seated comfortably while instructed to focus on an external fixed lamp. A CCD camera facilitated the precise attachment of a flat cover to the cornea. Following the established protocol, skilled inspectors utilized the "slice" option to capture horizontal central images of the cornea beneath the basal plexus. We employed the validated automated version of ACCMetrics to evaluate 4-6 CCM images, representing the highest image quality for each eye in the central corneal region (ACCMetrics, M.A. Dabbah, Imaging Science, University of Manchester, 2010). These parameters were measured and assessed based on previous findings, particularly with reference to established benchmarks[14, 15].

Corneal nerve feature extraction and SuStaIn modeling

Corneal nerve feature extraction

Corneal nerve features were automatically extracted using the validated ACCMetrics software. Images acquired from the central corneal region of each eye were analyzed in batch mode to identify corneal nerve fiber morphology and spatial distribution, followed by quantitative computation of nerve-related metrics. Six core corneal nerve features were retained for subsequent analysis: corneal nerve fiber density (CNFD), corneal nerve branch density (CNBD), corneal nerve fiber length (CNFL), corneal total branch density (CTBD), corneal nerve fiber area (CNFA), and corneal nerve fiber fractal dimension (CNFra).

Z-score normalization relative to healthy controls

To account for scale differences across features, all corneal nerve metrics were standardized relative to the healthy control group. For the i-th Parkinson's disease patient and the j-th feature, the Z-score Z_{ij} was calculated as:

$$Z_{ij} = \frac{X_{ij}^{PD} - \mu_j^{HC}}{\sigma_j^{HC}},$$

where X_{ij}^{PD} denotes the raw quantitative value of the j-th feature for patient i, μ_j^{HC} denotes the mean of the corresponding feature in healthy controls, and σ_j^{HC} denotes the standard deviation.

Definition of abnormality levels

Feature abnormality levels were defined as $m \in \{1,2,\cdots,K\}$, where K denotes the total number of abnormality grades. In this study, $K = 3$, corresponding to no obvious abnormality ($m = 1$), mild abnormality ($m = 2$), and severe abnormality ($m = 3$).

For each feature j, the 95th percentile of its Z-score distribution was denoted as z_j. Abnormality levels were assigned according to the following criteria:

- $m = 1$ when $Z_{ij} < z_j/3$;
- $m = 2$ when $z_j/3 \leq Z_{ij} < 2z_j/3$;
- $m = 3$ when $Z_{ij} \geq 2z_j/3$.

This grading scheme enables a coarse-to-fine representation of feature abnormality severity while preserving consistency across biomarkers.

Construction of the feature event matrix

Based on the abnormality grading results, a feature event matrix S was constructed as:

$$S \in [0,1]^{I \times J \times K},$$

where I denotes the number of Parkinson's disease patients, J denotes the number of core features, and K denotes the number of abnormality levels. Each element S_{ijk} indicates whether the j-th feature of patient i corresponds to abnormality level K, defined as:

$$S_{ijk} = \begin{cases} 1, & \text{if } m = k; \\ 0, & \text{if } m \neq k. \end{cases}$$

The feature event matrix provides an event-based representation of individual abnormality patterns and serves as a key input to the SuStaIn model.

SuStaIn model construction and training

The SuStaIn model was constructed using the feature event matrix S together with the patient feature Z-score matrix, which is an $I \times J$ matrix. Core model parameters were specified in advance, including the number of patients, number of features, maximum candidate number of subtypes, number of MCMC sampling iterations, number of random starting points, and number of cross-validation folds.

Independent model training was performed for each candidate subtype number up to the predefined maximum. For each candidate model, the ordering of feature abnormality events was optimized to maximize the model's likelihood with respect to the observed data.

MCMC-based uncertainty estimation of event ordering

To quantify uncertainty in the inferred ordering of feature abnormality events, Markov Chain Monte Carlo (MCMC) sampling was performed. For each feature j and abnormality level m, MCMC sampling generated a collection of event position samples:

$$E = \{\theta_{jm}^{t}\}_{t=1}^{T},$$

where θ_{jm}^{t} denotes the event position obtained at the t-th iteration and T denotes the total number of MCMC samples.

The mean event position was computed as:

$$\bar{\theta}_{jm} = \frac{1}{T}\sum_{t=1}^{T}\theta_{jm}^{t},$$

with the corresponding position variance and standard deviation calculated as:

$$s_{jm}^{2} = \frac{1}{T-1}\sum_{t=1}^{T}\left(\theta_{jm}^{t} - \bar{\theta}_{jm}\right)^{2},\ s_{jm} = \sqrt{s_{jm}^{2}}.$$

Only event position estimates satisfying predefined convergence and stability criteria were retained for subsequent subtype and stage inference.

Subtype and stage inference

Using the validated MCMC-derived statistics and model outputs, an input dataset was constructed as:

$$D = \left(\bar{\theta}_{jm}, s_{jm}^2, s_{jm}, S_{ijk}, Z_{ij}\right).$$

For patient i, the posterior probability P_{ipq} of belonging to subtype p at disease stage q was calculated according to:

$$P_{ipq} \propto P\left(S_{ijk}, Z_{ij} | \bar{\theta}_{jm}, s_{jm}^2, p, q\right) \cdot P(p, q),$$

where the prior probability was defined as:

$$P(p, q) = \frac{1}{R \cdot Q},$$

with R denoting the number of subtypes and Q denoting the number of disease stages per subtype.

Posterior probabilities were computed across all patients, subtypes, and stages. For each patient, the subtype and disease stage corresponding to the maximum posterior probability were selected as the final assignment, yielding the subtype–stage result set:

$$A = \left\{(i, p^*, q^*) | i \in \{1,2,\cdots, I\}\right\}.$$

Model selection

For each candidate subtype number p, the corresponding cross-validation information criterion $CVIC_p$ and log-likelihood value $LogL_p$ were extracted. These metrics were combined to form the indicator set:

$$F = \left\{\left(p, \mathrm{CVIC}_p, \mathrm{Log}L_p\right) | p = 1,2, \cdots, R\right\}.$$

The candidate subtype number associated with the minimum $CVIC_p$ was selected as the optimal model. When multiple candidate models exhibited identical $CVIC_p$ values, the model with the largest $LogL_p$ was selected.

Statistical analysis

The Shapiro-Wilke test was used to evaluate the normality of the data. When the variable follows a normal distribution, the data is expressed as mean ± standard deviation (SD); when the variable is not normally distributed, the data is expressed as median. Independent sample t-tests or non-parametric tests were used for comparison between the two groups. All statistical analyses were completed using SPSS version 22.0 software (developed by IBM in Armonk, New York State, USA). In addition, the data visualization adopts the products of GraphPad Software Company in San Diego, California, USA. The violin graph is generated through Graphpad Prism8.0 version software.

Result

Subtype and stage inference

SuStaIn determines the number of subtypes that the available data can support, reconstructs the stage trajectory within each subtype, and assigns the probability of each subtype and stage to each subject. These characteristics provide insights into the biology of potential diseases and the mechanisms of fine-grained stratification within the body in the early stages of diseases. We applied SuStaIn to plot the differences of each CCM index between the PD group and the HC group, analyzed the degree of change and trend of each index relative to the HC group, and deleted the inconsistent trend indicators. Then, the subtype graph selection method was adopted, with the maximum number of subtypes set at 4. Combined with the information index (CVIC value) and the log-likelihood value for comprehensive evaluation, two subtypes were finally determined as the optimal.(Figure 2)

Subtype progression pattern

We used various indicators of corneal nerve fibers from PD patients to demonstrate the role of SuStaIn in PD. This model classifies PD patients into two subtypes, namely subtype 1 (n=49 cases) and subtype 2 (n=16 cases). The model uses Z-scores to represent the degree of change in the characteristics of the PD group compared to the healthy control group. We distinguish the severity of the Z-scores by different colors (gradually increasing in the order of red, purplish red, and blue). Through the color map, we found that the CNFD, CNBD, CNFL, and CTBD indicators of type 2 changed earlier than those of type 1, indicating that type 2 accumulated

corneal nerve fibers earlier. However, the time when the CNBD and CTBD indicators reached blue was earlier in type 1 than in type 2, suggesting that type 1 progressed more rapidly. Therefore, we conclude that the model dynamics parameters reveal the distinct disease progression patterns of these two subtypes. Specifically, patients with subtype 1 exhibit a "delayed-rapid" progression pattern. The onset of corneal involvement is relatively late, but once it occurs, the rate of nerve fiber damage and loss is significantly faster. In contrast, patients with subtype 2 exhibit an "early-onset - slow" progression pattern, meaning that the cornea is already affected in the early stage of the disease, but the subsequent progression of nerve fiber damage is extremely slow. Descriptive analysis of the distribution of subtype populations further revealed that patients of subtype 1 were mainly concentrated in the early stage of the disease (H-Y stage 1-2.5, n=38), while the distribution of patients of subtype 2 was more uniform in each disease stage. (Figure 3)

SuStaIn reveals the subtypes and stages of the disease in PD

We compared and analyzed the corneal data of the two subtypes classified by SuStaIn. We found that subtype 1 CNFD (20.34±6.74 vs 30.28±5.33, $p<0.05$) and CNBD (21.87 (9.37, 27.60) vs 49.48 (44.84,63.28) The three indicators of $p<0.05$ and CNFL (12.30 (9.86, 13.49), $p<0.05$) were all significantly higher than those of subtype 2. Therefore, we consider subtype 1 to be severe corneal nerve fiber injury and Subtype 2 to be mild corneal nerve fiber injury. Similarly, this model divides the disease progression of PD patients into 12 stages based on the degree of corneal damage, from mild to severe, so as to quickly determine the disease progression stage of the patients at any stage. (Figure 4)

Characteristics of the Identified Subtypes

There were no significant differences between the two subtypes in terms of gender, age, disease duration, etc (Table 1). Compared with subtype 2, subtype 1 performed more severely in the scores of UPDRS-II (16.00 (8.50, 22.50) vs 9.50 (5.00, 13.75), $p < 0.05$), Frozen Gait Questionnaire (FOG) (13.00 (2.00, 18.00) vs 1.50 (0.00, 12.75), $p < 0.05$), and RBD-HK (34.00 (11.00, 40.50) vs 0.00 (0.00, 36.25), $p < 0.05$) (Figure 4). In addition, subtype 1 was more severe in corneal injury than subtype 2, that is, in CNFD, CNBD and CNFL, subtype 1

was significantly less than subtype 2 ($P< 0.05$). There was no statistically significant difference in these indicators such as UPDRS-I, UPDRS-III, UPDRS-IV, BERG Balance Scale (BERG), Montreal Cognitive Assessment (MoCA), and Autonomous Function Scale (SCOPA-AUT) between the two subtypes. Although there was no significant difference in the SCOPA-AUT scale between the two subtypes, the average degree of autonomic nerve function impairment in patients with subtype 1 was more severe than that in patients with subtype 2. (Figure 5)

Discussion

This study utilized the SuStaIn model to classify Parkinson's disease patients into two progression trajectories, namely "severe (subtype 1)" and "mild (subtype 2)", based on the degree of corneal nerve fiber damage. It also verified the significant differences between the two in terms of onset timing, progression rate, and clinical phenotype, providing a new peripheral-central dialogue perspective for the study of PD heterogeneity. The model inference results show that although the cornea of subtype 2 patients is affected early, the subsequent neurodegenerative spread is slow, suggesting that it may represent an "early-onset - slow-progression phenotype". On the contrary, although corneal damage occurs later in patients with subtype 1, it accelerates explosively, suggesting that it is closer to the "late-onset - rapid progression phenotype". More importantly, this study incorporated corneal confocal microscopy (CCM) parameters into the SuStaIn model, discovered subtypes that might be similar to the progression of PD pathological protein transmission patterns, and demonstrated that the peripheral small fiber damage trajectory can occur synchronously with central degenerative events, thereby truly pushing the "corneal window" to the practical level of individualized PD staging.

This study suggests that compared with subtype 2, the freezing gait (FOG) symptoms of subtype 1 are more severe. Combining the pathogenesis of frozen gait, FOG is regarded as a relatively independent and complex symptom domain in Parkinson's disease. A large amount of current evidence indicates that there is a poor response of FOG to levodopa and DBS. Therefore, FOG is not only the result of dopaminergic system dysfunction, but also the result of the participation of non-dopaminergic (cholinergic) mechanisms. Its pathophysiological

mechanism goes beyond the mere failure of the substantia nigra - striatum dopaminergic pathway. Previous studies have shown that FOG is closely related to the degeneration of cholinergic neurons in the cholinergic system, especially in the basal forebrain (NBM) and the pontine tegmental nucleus (PPN), particularly the degeneration of the frontal lobe-pontine cholinergic pathway involved in gait and attention control. FOG patients are more prone to attacks under distraction or dual tasks, suggesting the failure of cholinergic regulation. Cholinergic neurons in the pontine tegmental nucleus (PPN) and basal forebrain (NBM) start to be lost at the Braak α -synuclein stage 2-3. Their axons project to the thalamus, striatum and central pattern generator of the spinal cord, serving as the "pacemaker" for the automation of gait rhythm. Tavakoli et al. found through 18F-FEOBV PET that the density of cholinergic endings in the thalamus, pons tetragus (PPN), and hippocampus of PD patients with FOG was significantly decreased, and the extent of decrease was negatively correlated with the FOG questionnaire score ($r = -0.62$, $p < 0.001$). It is suggested that cholinergic deneurasthenia in the target area is a neurochemical substrate produced by FOG[16].Image-electrophysiology further demonstrated that in patients with early FOG, the volume of gray matter in the left cuneus, lingual gyrus and posterior cingulate cortex decreased, which was parallel to the decline in the resting-state functional connectivity of the parietal insular lobe, reflecting the premature damage of the visual-vestibular - proprioceptive integration network, and this area is precisely where cholinergic axons are densely distributed. Therefore, we believe that the FOGQ difference between subtype 1 and subtype 2 supports the "cholinergic - brainstem - frontal lobe" circuit as a potential pathophysiological basis for the subtype of severe corneal nerve injury and plays a key role in the delayed-rapid progression phenotype. So, why is this circuit particularly related to corneal nerve damage? The key lies in the unique cholinergic dependence of the cornea itself. The cornea is the tissue with the densest nerve innervation in the body. One of its nerve sources is the trigeminal ganglion, which receives parasympathetic cholinergic nerve fiber branches from the pterygopalatine ganglion and is responsible for regulating tear secretion, corneal nutrition and local immune homeostasis. This indicates that the health and function of corneal nerve fibers themselves depend on cholinergic signaling[17, 18]。 Previous studies on diseases such as Alzheimer's disease and Parkinson's disease have all shown a significant decrease in corneal nerve parameters, and these diseases all involve dysfunction of the

cholinergic system[19, 20].Therefore, an increasing number of researchers believe that the health of the corneal nerve depends on the cholinergic instructions issued by the central nervous system. When the central cholinergic system degenerates, secondary damage to the corneal nerve may occur[21, 22].This is consistent with our team's previous research results, that is, there is a correlation between corneal nerve parameters and the severity of frozen gait[23]. It may serve as a peripheral marker of cholinergic degeneration in the response center. Therefore, we believe that the changes in corneal nerves may be the peripheral mirror image of cholinergic degeneration. Then, the sharp decline in corneal nerve fiber density (CNBD), corneal nerve fiber length (CNFL), and branch density (CNBD) of subtype 1 patients in this study can be regarded as the peripheral mirror image of "systemic cholinergic vulnerability". Combined with the significant FOG that occurred early in this subtype, it is speculated that there may be synchronous degeneration of the "frontal lobe - pons cholinergic white matter bundle" in this subtype. This leads to the failure of attention-gait coupling.

At present, the pathological classification of PD is mainly summarized into two patterns based on the dissemination direction of α-synuclein: "body first" and "brain first". The former invays the medulla oblongata from the reverse axons of the intestinal or peripheral autonomic nerves and then ascends to the substantia nigra and cortex. The latter starts from the olfactory bulb or basal forebrain and progresses to the tail substantia nigra - striatum and cortex. Peripheral involvement occurs relatively late[24, 25].Under this framework, the synchronous degeneration of the "frontal lobe - pontine cholinergic white matter bundle" presented by subtype 1 of this study, which shows a significant sharp drop in corneal nerve fiber density, length and branch density, precisely corresponds to the core feature of the "peripheral cholinergic - sympathetic axis" first involved in the body-first type α-synuclein. The early and severe RBD is also consistent with the early involvement of the medulla oblongata vagus-nucleus and ventral reticular structure, while the late-onset - rapid progression phenotype reflects a "bottom-up" dissemination rhythm from the periphery → brainstem → substantia nigra. In the body-first type, motor symptoms show a tendency to progress more rapidly and severely, which is consistent with the more severe FOG reflected in subtype 1 of this study. This is a direct manifestation of the disintegration of the pons tegmental - basal forebrain - frontal cholinergic

circuit, rather than being explained by the simple deficiency of dopamine in the substantia nigra - striatum[26]. Previous studies have suggested that the pathological proteins of the "body-first" subtype can involve peripheral nerve fibers at an early stage. However, subtype 1 in this study is characterized by delayed damage to corneal nerve fibers. This contradictory phenomenon implies that although the pathological process initiates in the early peripheral stage, corneal nerves are insensitive to pathological proteins, and pathological proteins preferentially travel along the main vagus nerve pathway to the brainstem. Significant damage to the corneal nerve may only become apparent when pathological proteins accumulate to a certain extent; once it occurs, it progresses rapidly. Therefore, subtype 1 can be regarded as a special variant of the body-first type on the corneal small nerves, serving as a peripheral "biological imprint" of the body-first type and possibly as a peripheral screening tag for "rapid degeneration of central cholinergic function", providing a basis for the early activation of cholinesterase inhibitors or deep electrical stimulation targeting PPN.

It is worth noting that the vast majority of patients in subtype 1 are still in the early stage of this subtype, but the FOG score is significantly higher than that of subtype 2. This exposure is first attributed to the threshold effect of the frontal lobar - pons cholinergic circuit on gait-attention coupling: a slight decrease in cholinergic synaptic density can cause instability of the corticostem "gate" during dual tasks or turning, resulting in transient motor block. This discovery is highly consistent with the SuStaIn study based on DAT-SPECT by Nalls et al. They also found that the "rapid presynaptic dopamine deficiency type" subtype could present with postures instability and aggravated RBD in the early stage of imaging. The core biological basis of this subtype is the rapid loss of dopaminergic neurons, accompanied by extensive degeneration of the cholinergic system, that is, the synchronous collapse of the cholinergic-brainstem network can occur in the early stage of the disease. This discovery suggests that the SuStaIn model can identify high-risk progressive populations at stages that are "not yet captured by classical scales"[27].Furthermore, this study found that there were also significant differences in UPDRS-II between the two subtypes. Since the degree of frozen gait (FOG) and RBD in patients with subtype 1 is more severe, both of which are direct driving factors for the increase of UPDRS-II. FOG leads to difficulty in starting gait, freezing when turning and fear of falling,

directly increasing the scores of both "walking" and "falling". RBD reduces patients' willingness to be active and their execution efficiency through sleep fragmentation, daytime sleepiness and fatigue, indirectly accelerating functional decline. Furthermore, cholinergic system damage is one of the core mechanisms of the "body-first" subtype. The loss of cholinergic neurons in the basal forebrain not only mediates RBD and cognitive fluctuations but also makes patients more prone to gait freeze and attention collapse in dual-task or complex environments, thereby further weakening their ability to live independently. More importantly, the "rapid progression" feature of Subtype 1 shortens the functional compensation window. At the same disease course node, the degree of disability has exceeded subtype 2, resulting in the amplification of the difference in UPDRS-II scores. This is consistent with the previous research results of Seyed-Mohammad Fereshtehnejad, who found that the "diffuse malignant" subtype had a higher UPDRS-II score at baseline, and during the follow-up period, its UPDRS-II deterioration rate was the fastest, accompanied by faster cognitive decline and a higher degree of disability[28]. Therefore, UPDRS-II not only reflects the current functional impairment but can also be regarded as a "clinical mirror image" of the rapid progression of subtype 1. S-M et al. also found that there was no statistically significant difference in the total score of the motor Examination (UPDRS-III) between the "diffuse malignancy" subtype and the "mild exercise-dominant" subtype, which is consistent with the results of this study. In this study, subtype 1 and subtype 2 showed significant differences in the indicators reflecting cholinergic impairment. However, no difference was observed in the total score of UPDRS-III, which is mainly regulated by the dopaminergic system. This result highlights the limitations of the total score of UPDRS-III in identifying non-dopaminergic pathological differences. The official validation literature of this scale indicates that the symptoms such as postures instability and gait disorders included in its third part themselves have relatively weak responses to dopaminergic treatment, suggesting that its pathophysiological basis involves non-dopaminergic systems such as cholinergic. Therefore, as a comprehensive indicator, the total score of UPDRS-III is mainly dominated by the items sensitive to dopaminergy, and it may be difficult to effectively capture the specific damage differences in non-dopaminergic pathways among different subtypes[29].

The mean value of subtype 2 on the cognitive scale is better than that of subtype 1, and the

SCOPA-AUT score is lower, suggesting that the autonomic neuro-cognitive network is less affected. This suggests that the pathological load may still be concentrated in the olfactory cortex circuit and has not widely affected the peripheral sympathetic nerve and brainstem gait center. This pathological dissemination path is consistent with the "brain-first" type. It is speculated that the α -synuclein lesion spreads retrograde from the cortex to the brainstem. Pathology may spread very early from the starting point (such as the olfactory bulb) to the brainstem region that is anatomically and functionally adjacent to it (for example, the region associated with the sensory nucleus of the trigeminal nerve). Once the trigeminal nerve nuclei in the brainstem are involved, pathological proteins can be transported longitudinally through axons and directly reach the trigeminal ganglion and corneal nerve endings[30]. Therefore, as a special sensory nerve innervated by cranial nerves, the corneal nerve may belong to a "proximal peripheral" area that is extremely closely connected to the central nervous system, and its involvement occurs much earlier than those "distal peripheral" areas (such as the autonomic nerves of the intestine and heart). The "early-onset" injury of subtype 2 precisely reflects the early involvement of this rapid and direct cranial nerve pathway. As the main driving engine and burden of the disease are still concentrated in the olfactory cortex circuit, the overall course of the disease progresses relatively slowly, and the damage to the corneal nerves also presents a pattern of "early onset but slow aggravation". This means that the corneal nerve, as a proximal part of the peripheral nerve, can be affected at an early stage. However, due to the slow progression of central lesions and their main concentration in specific areas, the overall impact on the peripheral nerve is relatively small, resulting in a slow progression of corneal nerve injury. The trajectory of the "early-onset - slow" progression pattern of subtype 2 conforms to this pathological transmission process. Combining the feature of "uniform distribution in each stage" of SuStaIn, this phenotype of "early cortical symptoms, mild peripheral symptoms, and slow progression slope" is highly consistent with the time sequence and anatomical dissemination direction of the "brain-first" model. It can be speculated that subtype 2 May correspond to the slow variant under the "brain-first" hypothesis, that is, the retrograde transmission of the α -synuclein disease from the cortex to the brainstem. Its compensatory mechanisms (such as cortical plasticity or glial-lymphatic clearance) delay functional breakdown. Guttuso et al. conducted a one-year follow-up on 104 patients with early PD and

found that the annual increase rate of free water in the dorsolateral thalamic nucleus was significantly negatively correlated with the decrease of MoCA during the same period ($r = -0.22$, $q < 0.05$), suggesting that this indicator can capture cognitive network degeneration before significant changes in clinical scales[31]. Ofori et al. further pointed out that the free water in the substantia nigra increases linearly over time, and its rate is synchronous with the deterioration amplitude in UPDRS-III years, indicating that free water imaging is also applicable to the quantification of the progression of the movement axis. Based on the above cohort data, it can be inferred that if there is a PD subtype with "cognitive retention and slow motor progression", the annual change rate of free water in the corpus callosum knee and cingulate fasciculus should be significantly lower than that in the rapid progression group. This "image-clinical" separation phenomenon provides verifiable imaging biomarkers for white matter structure compensation to delay functional deterioration, and also offers indirect support at the central level for our "mild trajectory" based on corneal parameter classification. Although the corneal nerve was involved in the early stage, it showed a "low slope" decline due to the relatively mild rate of central degeneration, thus providing living evidence for the hypothesis of "corneal and central synchronous but different rates"[32].

The limitation of this study lies in that although the potential association between corneal neuropathy and the dysfunction of the central cholinergic system in Parkinson's disease was explored, the central cholinergic endings were not directly determined. Although there is evidence that cholinergic neurotransmitters play a role in corneal nerve regulation, and diseases involving cholinergic system dysfunction such as Parkinson's disease are all accompanied by a significant decrease in corneal nerve parameters, the lack of direct central measurement data makes this association still need further direct evidence to strengthen. In the future, this hypothesis can be verified through more direct biomarkers or imaging methods.

Conclusion

This study, integrated corneal confocal microscopy with the SuStaIn model, successfully identifying two progressive subtypes of Parkinson's disease. Subtype 1 (delayed-rapid progression type) is characterized by late corneal involvement and rapid deterioration, which is

associated with the "body-first" transmission pattern and central cholinergic damage, leading to significant freezing of gait. In contrast, Subtype 2 (early-onset - slow-progression type) exhibits early corneal involvement but progresses slowly, aligning with the "brain-first" model. This discovery underscores the importance of corneal parameters in analyzing the heterogeneity of Parkinson's disease and offers a novel approach for individualized disease staging through a "peripheral-central" combined analysis.

Authorship contribution statement

Chenyang Guan: Writing original draft, Methodology, Conceptualization. Zixuan Wu: statistical analysis, Draw a type diagram. Liying Yang: Writing review & editing, Resources. Xiaojie Qim, Zihao Lin, Yating Fang, Zhuoxuan Yu, KUPPAM SAI SAGAR, SHAHRUKH KHAN, Yangdanyu Li, Peixiao Yin, YTXuebin Niu: Data collection, Project administration. He Wang, Lu Chen: Ophthalmic testing. Jing Liu, Guiyun Cui: Writing original draft, Visualization. Lishun Xiao: Software, Data curation. Kun Zan: Writing review & editing, Resources. Chuanying Xu: Visualization, Validation.

Ethics approval

The study was approved by the Ethics Committee of the Affiliated Hospital of Xuzhou Medical University (XYFY2022-KL 227–01 / XYFY2023-KL 265-01 / XYFY2024-KL541-01), and each participant provided informed consent. The study followed the principles of the Declaration of Helsinki regarding the clinical investigation of human subjects.

Funding

The paper is supported by: (1) National Natural Science Foundation of China (82401683) (2) Advanced Program of The Affiliated Hospital of Xuzhou Medical University(PYJH2024316) (3) Construction Project of High Level Hospital of Jiangsu Province (GSPJS202424).

Declaration of competing interest

The authors declare no conflict of interest.

Acknowledgments

We thank the patients for their participation and their families for their cooperation in this study. We also thank the Manchester Biomedical Research Centre for access to the ACCMetrics

software. This work was supported by the staff of the Xuzhou Medical University Hospital Parkinson's team.

Data availability statement

This article contains all of the data collected or analyzed during the course of this investigation. Further inquiries should be made to the relevant author.

References

[1] Seibler P, Streubel-Gallasch L and Klein C. Combining Biomarkers with Genetics In Prodromal/Earliest Phase Parkinson's Disease[J]. *Journal of Parkinson's disease*, 2024, 14(s2): S345–s351.
[2] Lee SH, Park SM, Yeo SS et al. Parkinson's Disease Subtyping Using Clinical Features and Biomarkers: Literature Review and Preliminary Study of Subtype Clustering[J]. *Diagnostics (Basel, Switzerland)*, 2022, 12(1).
[3] Liu M, Wen T, Luo H et al. Distinct cutaneous α-synuclein signatures in body-first and brain-first Parkinson's disease subtypes[J]. *Brain : a journal of neurology*, 2025.
[4] Li X, Chen C, Pan T et al. Trends and hotspots in non-motor symptoms of Parkinson's disease: a 10-year bibliometric analysis[J]. *Frontiers in aging neuroscience*, 2024, 16: 1335550.
[5] Müller LJ, Marfurt CF, Kruse F et al. Corneal nerves: structure, contents and function[J]. *Exp Eye Res*, 2003, 76(5): 521–542.
[6] He J and Bazan HE. Neuroanatomy and Neurochemistry of Mouse Cornea[J]. *Invest Ophthalmol Vis Sci*, 2016, 57(2): 664–674.
[7] Beach TG, Adler CH, Sue LI et al. Multi-organ distribution of phosphorylated alpha-synuclein histopathology in subjects with Lewy body disorders[J]. *Acta Neuropathol*, 2010, 119(6): 689–702.
[8] Ortuño-Lizarán I, Beach TG, Serrano GE et al. Phosphorylated α-synuclein in the retina is a biomarker of Parkinson's disease pathology severity[J]. *Mov Disord*, 2018, 33(8): 1315–1324.
[9] Kuo YM, Li Z, Jiao Y et al. Extensive enteric nervous system abnormalities in mice transgenic for artificial chromosomes containing Parkinson disease-associated alpha-synuclein gene mutations precede central nervous system changes[J]. *Hum Mol Genet*, 2010, 19(9): 1633–1650.
[10] Lim SH, Ferdousi M, Kalteniece A et al. Corneal Confocal Microscopy Identifies Parkinson's Disease with More Rapid Motor Progression[J]. *Mov Disord*, 2021, 36(8): 1927–1934.
[11] Che NN, Jiang QH, Chen S et al. The severity of corneal nerve loss differentiates motor subtypes in patients with Parkinson's disease[J]. *Ther Adv Neurol Disord*, 2023, 16: 17562864231165561.
[12] Young AL, Marinescu RV, Oxtoby NP et al. Uncovering the heterogeneity and

temporal complexity of neurodegenerative diseases with Subtype and Stage Inference[J]. *Nature communications*, 2018, 9(1): 4273.
[13] Postuma RB, Berg D, Stern M et al. MDS clinical diagnostic criteria for Parkinson's disease[J]. *Mov Disord*, 2015, 30(12): 1591–1601.
[14] Tavakoli M, Ferdousi M, Petropoulos IN et al. Normative values for corneal nerve morphology assessed using corneal confocal microscopy: a multinational normative data set[J]. *Diabetes Care*, 2015, 38(5): 838–843.
[15] Alam U, Jeziorska M, Petropoulos IN et al. Diagnostic utility of corneal confocal microscopy and intra-epidermal nerve fibre density in diabetic neuropathy[J]. *PLoS One*, 2017, 12(7): e0180175.
[16] Bohnen NI, Kanel P, Zhou Z et al. Cholinergic system changes of falls and freezing of gait in Parkinson's disease[J]. *Annals of neurology*, 2019, 85(4): 538–549.
[17] Al-Janahi E, Ponirakis G, Al Hamad H et al. Corneal Nerve and Brain Imaging in Mild Cognitive Impairment and Dementia[J]. *J Alzheimers Dis*, 2020, 77(4): 1533–1543.
[18] Marfurt CF, Cox J, Deek S et al. Anatomy of the human corneal innervation[J]. *Exp Eye Res*, 2010, 90(4): 478–492.
[19] Che NN, Jiang QH, Ding GX et al. Corneal nerve fiber loss relates to cognitive impairment in patients with Parkinson's disease[J]. *NPJ Parkinson's disease*, 2021, 7(1): 80.
[20] Ponirakis G, Hamad HA, Khan A et al. Loss of corneal nerves and brain volume in mild cognitive impairment and dementia[J]. *Alzheimers Dement (N Y)*, 2022, 8(1): e12269.
[21] Ramos-Martínez IE, Rodríguez MC, Cerbón M et al. Role of the Cholinergic Anti-Inflammatory Reflex in Central Nervous System Diseases[J]. *Int J Mol Sci*, 2021, 22(24).
[22] Winek K, Soreq H and Meisel A. Regulators of cholinergic signaling in disorders of the central nervous system[J]. *J Neurochem*, 2021, 158(6): 1425–1438.
[23] Guan C, Xu X, Yin P et al. The role and molecular mechanism of α synuclein in Parkinson's disease: A diagnostic model for corneal nerve fiber injury[J]. *International journal of biological macromolecules*, 2025, 306(Pt 1): 141238.
[24] Borghammer P, Horsager J, Andersen K et al. Neuropathological evidence of body-first vs. brain-first Lewy body disease[J]. *Neurobiol Dis*, 2021, 161: 105557.
[25] Passaretti M, Veréb D, Mijalkov M et al. Clinical progression and genetic pathways in body-first and brain-first Parkinson's disease[J]. *Mol Neurodegener*, 2025, 20(1): 74.
[26] Braak H and Del Tredici K. Neuropathological Staging of Brain Pathology in Sporadic Parkinson's disease: Separating the Wheat from the Chaff[J]. *Journal of Parkinson's disease*, 2017, 7(s1): S71–s85.
[27] Zhou C, Wang L, Cheng W et al. Two distinct trajectories of clinical and neurodegeneration events in Parkinson's disease[J]. *NPJ Parkinson's disease*, 2023, 9(1): 111.
[28] Fereshtehnejad SM, Romenets SR, Anang JB et al. New Clinical Subtypes of Parkinson Disease and Their Longitudinal Progression: A Prospective Cohort Comparison With Other Phenotypes[J]. *JAMA Neurol*, 2015, 72(8): 863–873.
[29] Goetz CG, Tilley BC, Shaftman SR et al. Movement Disorder Society-sponsored revision of the Unified Parkinson's Disease Rating Scale (MDS-UPDRS): scale

presentation and clinimetric testing results[J]. *Mov Disord*, 2008, 23(15): 2129–2170.
[30] Borghammer P. The α-Synuclein Origin and Connectome Model (SOC Model) of Parkinson's Disease: Explaining Motor Asymmetry, Non-Motor Phenotypes, and Cognitive Decline[J]. *J Parkinsons Dis*, 2021, 11(2): 455–474.
[31] Guttuso T, Jr., Sirica D, Tosun D et al. Thalamic Dorsomedial Nucleus Free Water Correlates with Cognitive Decline in Parkinson's Disease[J]. *Movement disorders : official journal of the Movement Disorder Society*, 2022, 37(3): 490–501.
[32] Ofori E, Pasternak O, Planetta PJ et al. Longitudinal changes in free-water within the substantia nigra of Parkinson's disease[J]. *Brain : a journal of neurology*, 2015, 138(Pt 8): 2322–2331.

Figure Legends

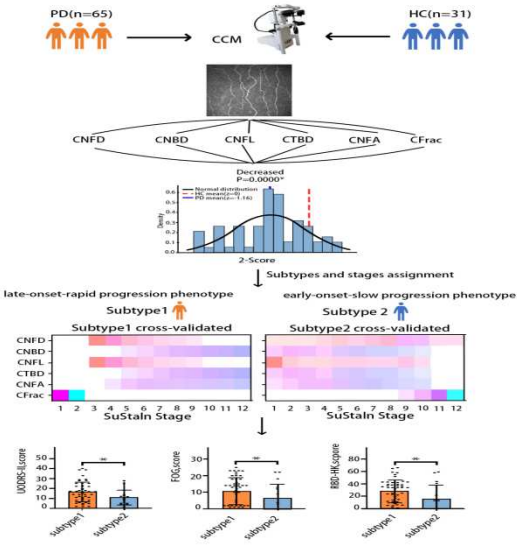


Figure 1 Experiment flowchart

A total of 82 individuals (65 in discovery dataset and 17 in validation dataset) were enrolled in this study; corneal nerve fiber parameters were used for model construction; these corneal parameter variables include CNFD, CNBD, CNFL, CTBD, CNFA, and CNFra.

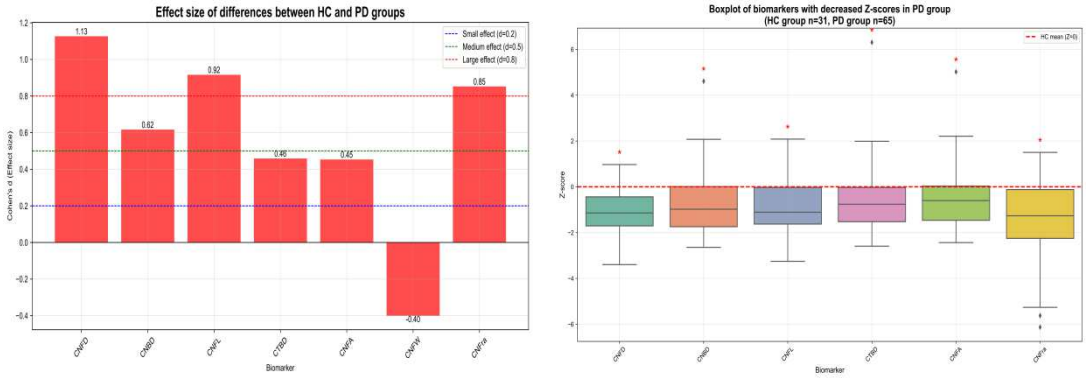
Table 1 Differences in demographics, clinical variables, and corneal parameters between subtypes

	subtype 1 (n=49)	subtype 2 (n=16)	P
Age, mean ± SD, years	66.47±7.04	67.25±7.45	0.705
Sex (M/F)	19/30	9/7	
Disease duration, years	4.00 (2.00, 7.50)	3.50 (2.00, 7.50)	0.866
Hoehn and Yahr Stage	2.00 (2.00, 2.50)	2.00 (2.00, 2.50)	0.474
UPDRS-I, score	10.00 (8.00, 16.50)	11.00 (8.25, 16.5)	0.708

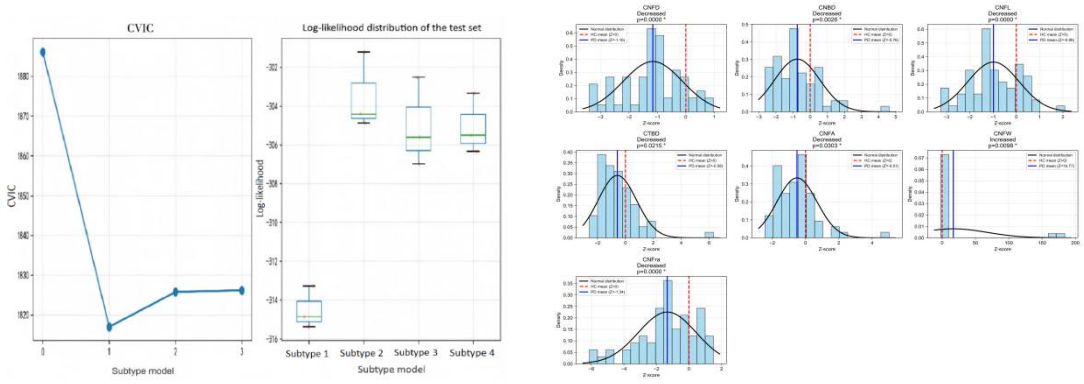
UPDRS-II, score	16.00 (8.50, 22.50)	9.50 (5.00, 13.75)	0.032*
UPDRS-III, score	35.00 (19.00, 43.50)	28.00 (15.75, 42.75)	0.402
UPDRS-IV, score	0.00 (0.00, 4.00)	0.00 (0.00, 4.75)	0.986
SCOPA-AUT, mean ± SD	17.39±10.53	15.13±9.12	0.444
FOG, score	13.00 (2.00, 18.00)	1.50 (0.00, 12.75)	0.031*
Berg, score	49.00 (42.50, 54.00)	53.50 (40.75, 54.00)	0.432
MOCA, score	20.00 (12.50, 26.00)	20.00 (19.00, 22.75)	0.778
RBDHK, score	34.00 (11.00, 40.50)	0.00 (0.00, 36.25)	0.017*
CNFD, mean ± SD, no./mm2	20.34±6.74	30.28±5.33	0.000***
CNBD, mean ± SD, no./mm2	21.87 (9.37, 27.60)	49.48 (44.84, 63.28)	0.000***
CNFL, mean ± SD, mm/mm2	12.30 (9.86, 13,49)	17.92 (16.67, 18.40)	0.000***

The data is presented as mean ± SD or median (interquartile range). To compare two groups of normally distributed variables, an independent sample t-test was performed. For variables with non-normal distributions or non-homoscedasticity, the nonparametric Mann-Whitney test was employed to compare two groups. The categorical variables were compared using chi-squared or Fisher's exact tests. CNBD, corneal nerve branch density; CNFD, corneal nerve fiber density; CNFL, corneal nerve fiber length; UPDRS, Unified Parkinson's Disease Rating Scale; SCOPA-AUT, the scale for outcomes in PD for autonomic symptoms; FOG, Freezing of Gait Scale; Berg, Berg Balance Scale; MOCA, Montreal Cognitive Assessment Scale; RBDHQ, The REM Sleep Behavior Disorder Screening Questionnaire Scale.

***p < 0.05 , **p < 0.01, ***p < 0.001**



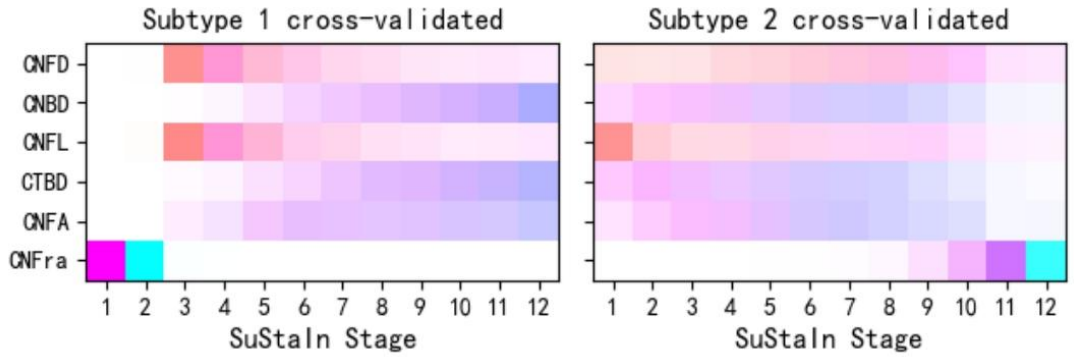
a **b**



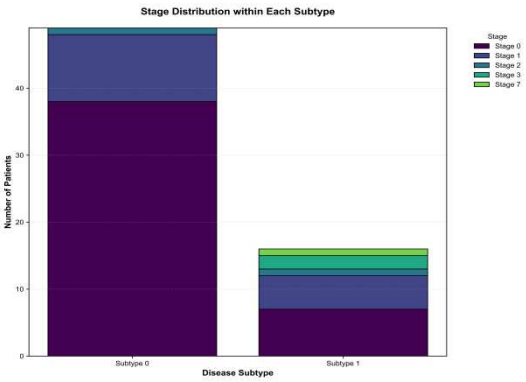
c **d**

Figure 2 Subtype construction

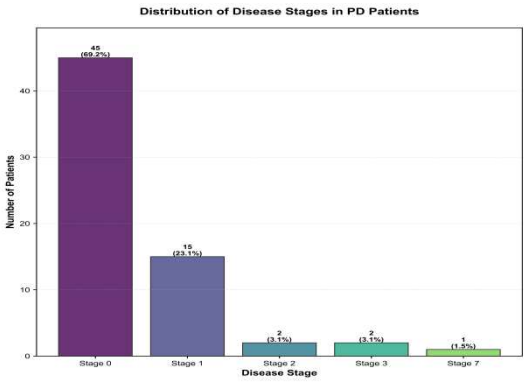
SuStaIn was applied to delineate the differences in CCM indices between the PD and HC groups, analyze the degree and trend of change for each index relative to the HC group, and eliminate indices with inconsistent trends. The maximum number of subtypes was set to 4, and subtyping was performed for 1, 2, 3, and 4 subtypes respectively, to determine which number of subtypes yielded the best effect. a. shows the differences in each corneal nerve fiber parameter between the HC and PD groups. The larger the absolute value of the effect size, the greater the difference between the HC and PD groups for this feature. b. is a visualization boxplot of the changes in Z-scores of each feature in the PD group relative to the healthy control group. c. Subtype selection diagram, the smaller the CVIC value, the better the classification result; the larger the log-likelihood value, the better the classification result. d. Distribution of Z-scores for corneal parameters, to quantify the degree of neurological damage in PD patients relative to healthy controls, this invention establishes a feature baseline using data from the HC group and calculates Z-scores using a standardization method to describe the degree of feature abnormality. For the j-th feature and the i-th patient, the Z-score is calculated according to the following formula: $Z_{ij}=\frac{X_{ij}^{PD}-\mu_j^{HC}}{\sigma_j^{HC}}$. X_{ij}^{PD} **represents the original feature values of PD patients;** μ_j^{HC} **represents the mean value of the feature in the HC group;** σ_j^{HC} **represents the standard deviation of the feature in the HC group; The larger the Z-score, the more significant the deviation of this feature in PD patients from the healthy controls, indicating more severe nerve fiber damage.**



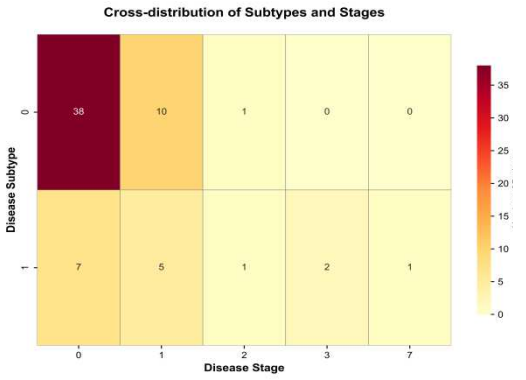
a



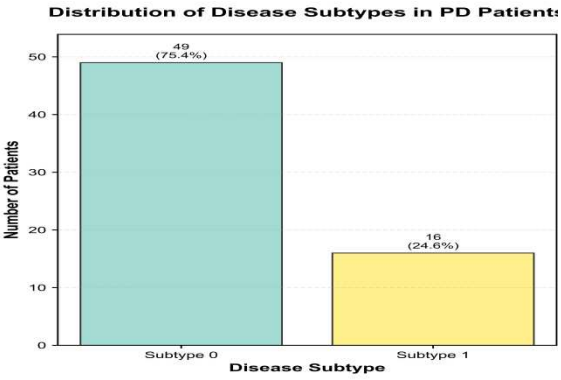
b



c



d



e

Figure 3 Order of event progression

a The model outputs a complete feature sequence diagram for each subtype, with colors ranging from red → purple → blue indicating the progression from mild to severe damage. b , c and e show the classification results of PD. d The stage distribution of patients in the two subtypes, In Subtype 1, the vast majority of patients are in the early stages; compared to Subtype 1, the stage distribution of patients in Subtype 2 is more even.

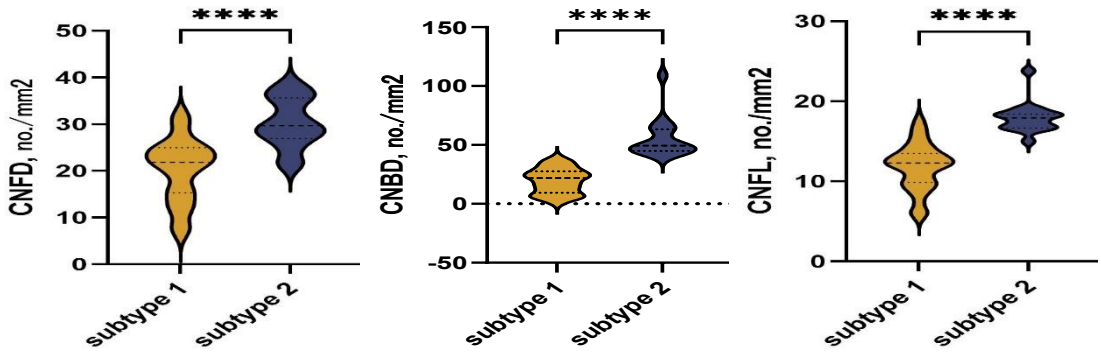


Figure 4 Comparison of corneal parameters between the two subtypes

Subtype 1, more severe corneal nerve fiber damage compared with subtype 2. Subtype 1, severe corneal nerve damage; Subtype 2, mild corneal nerve fiber damage; CNBD, corneal nerve branch density; CNFD, corneal nerve fiber density; CNFL, corneal nerve fiber length.

***p < 0.05; **p < 0.01; ***p < 0.001; ****p < 0.0001.**

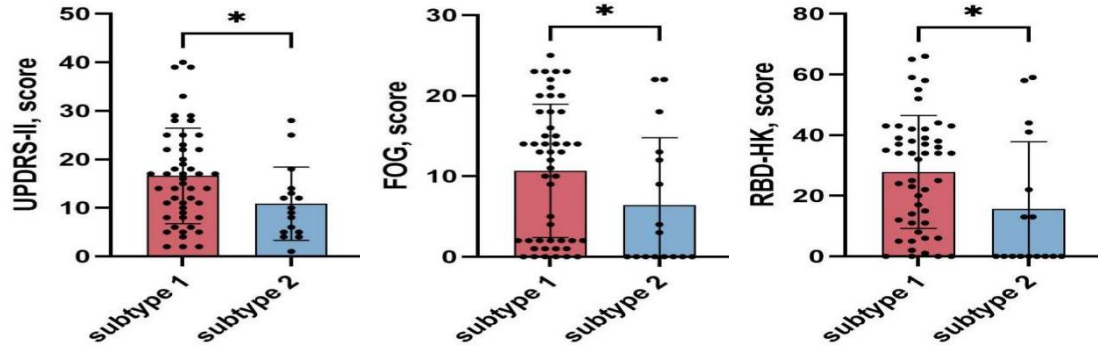


Figure 5 Comparison of clinical scales between the two subtypes

The differences in FOG, UPDRS-II and RBD-HK values between subtype 1 and subtype 2. Subtype 1, severe corneal nerve damage; Subtype 2, mild corneal nerve fiber damage; UPDRS, Unified Parkinson's Disease Rating Scale; FOG, Freezing of Gait Scale; RBDHQ, The REM Sleep Behavior Disorder Screening Questionnaire Scale.

***p < 0.05; **p < 0.01; ***p < 0.001; ****p < 0.0001.**